Advances in Continuous and Discrete Models

RESEARCH Open Access

Impact of the infected population and nonlinear incidence rate on the dynamics of the *SIR* model

Kuldeep Malik[1*] and Saad Althobaiti[2]

*Correspondence:
malik.kuldep@gmail.com
[1]School of Liberal Studies, Dr B. R. Ambedkar University, Lodhian Road, Delhi, 110006, Delhi, India
Full list of author information is available at the end of the article

Abstract

This study proposes a dynamical epidemic model *SIR* incorporating a nonlinear saturated incidence and nonlinear recovery rates. The model considers the influence of available resources, the ratio of the infected population, and the decrease of interventions on the spread of infectious diseases. The use of a nonlinear incident rate as a monoid-type equation improves the study compared to a constant-type incident rate because the spread of infection is now determined by the force of the illness and the number of infected individuals available to disseminate the infection. The consideration of recovery rate, which includes the minimum and maximum feasible recovery rates and the amount of resources available for treatment, makes the research more advantageous. The conditions for the existence of the equilibria have been established. Furthermore, stability analysis and bifurcation have been carried out using Lyapunov's direct method, the Routh–Hurwitz criterion, and Dulac's creation under each set of conditions. A numerical simulation was conducted using *MATLAB*. As the value of the preventive measure increases, the results indicate a considerable decrease in the infected compartment. In addition, the recovered population is growing as more resources, such as oxygen cylinders, hospital beds, and vaccination doses, become available.

Keywords: *SIR* model with nonlinear incident and recovery rate; Existence of Points of Equilibria; Stability analysis at equilibrium; Bifurcation analysis; Numerical simulation

1 Introduction

An epidemic is defined as an unanticipated disease outbreak that harms a significant portion of the habitat's population before it can be eradicated [1]. Epidemic outbreaks recur at intervals of many years elapsed between pandemics. An analysis of disease occurrence is called epidemiology. In addition to affecting millions of people, the widespread transmission of infectious diseases has a negative impact on social, political, economic, and geographic aspects of society [2]. In many countries around the world, infectious diseases such as cholera, malaria, and others are regarded as endemic. Certain diseases spread by viruses, such as influenza, while others spread by bacteria, such as tuberculosis, and still others spread by carriers, such as flies, ticks, mosquitoes, and so on, such as malaria. An

important tool for grasping the mechanisms underlying the spread and decline of infectious diseases is the epidemiological model. When gathering information through other channels like direct observation or experimentation is impractical, mathematical modeling might be helpful. Models are created using stochastic equations or ordinary differential equations. Since mathematical modeling of infectious disease transmission dynamics provides both short- and long-term forecasting of disease occurrence in the population and the reliance on multiple factors, it is crucial for a better understanding of epidemiological models and prevention and control strategies.

These days, mathematical modeling of an epidemic is a significant tool for comprehending, predicting, as well as controlling outbreaks of diseases. The concept of "mathematical modeling of an infectious disease" describes a deterministic method that uses differential equations to categorize the entire human population into compartments based on the presence or absence of infectious diseases. These compartments include susceptible population (S), infectious population (I), and recovered population (R). Movement within these compartments is caused by infection, progression, recovery, or migration. These variables show the number of individuals in every section at any particular moment. Here, S stands for the total number of people who are susceptible. A susceptible individual acquires the infection and joins the infected class when they come in contact with an infected individual. I stands for the total number of infected people. They are infectious and have the potential to spread the disease to susceptible populations; R is the proportion of individuals who are resistant or have recovered. These individuals were infected and have either recovered from their disease, shifted to a different class, or passed away.

In mathematical epidemiology, the *SIR* model proposed by Kermack and McKendrick in 1927 was crucial [3]. The effects of significant dynamics were first presented by Kermack and McKendrick (1932) in subsequent work [4]. The model's uses and summary were provided by Hethcote in 1976 [5].

$N = S + I + R$ represents the entire human population, and N is assumed to be constant during the simulation. The model that Kermack and Mckendrick (1927) proposed is as follows:

$$\begin{aligned} \frac{dS}{dt} &= -\beta SI, \\ \frac{dI}{dt} &= \beta SI - \alpha I, \\ \frac{dR}{dt} &= \alpha I, \end{aligned} \tag{1}$$

where β and α represent the infection and recovery rate, respectively, of the individuals who are infected.

Numerous models of epidemics have been proposed in the literature. Agarwal and Verma [6] examined the saturating contact rate of contacts of a person provided by Heesterbeek and Metz [7] and developed an epidemic model *SIR*. The dynamics of an infectious-disease model is mostly determined by the function that characterizes the incidence rate. In epidemiological models [1, 2, 8, 9], where the dynamics are merely established by the basic reproduction number, $\Re_0$, standard bilinear incidence rate, αIS, has been utilized frequently. If $\Re_0 < 1$, the disease will vanish and all populations will become susceptible; if not, it will continue. The influence of prevention tactics like mask wearing, self-isolation, and quarantine, which are crucial in containing the spread of infectious

illnesses, is not taken into account in the calculation of those bilinear incidence rates. Therefore, it is imperative to take note of the impact of intervention tactics and the progressive reduction of interventions on the transmission of infectious diseases. In [10–12] some mathematical models are examined that handled corona infection using mathematical models.

Several researchers took into account various forms of incidence rate in their works. The saturated incidence rate $\frac{\alpha IS}{1+\beta I}$, for instance, was first described by Anderson and May [2] in 1978. It saturates as a result of the concentration of infectious individuals at high infection levels. $\frac{\alpha IS}{1+\beta_1 S+\beta_2 I}$ is an additional nonlinear incidence rate that was separately introduced by DeAngelis [13] and Beddington [14]. This incidence rate underwent modification, and $\frac{\alpha IS}{1+\beta_1 S+\beta_2 I^2}$ with a nonlinear recovery rate was employed by Gui-Hua Li and Yong-Xin Zhang [15]. The incidence rate responds more slowly to a gradual decline in intervention tactics than it would to a conventional bilinear term, αIS. Conversely, a higher rate of rise than bIS may be observed if few intervention measures are used. Government interventions have a significant negative influence on the economy as a consequence of pandemics like COVID-19. These initiatives have increased unemployment rates and corporate bankruptcy cases, which has caused governments to limit their level of intervention [16–19].

In order to examine the impact of intervention decrease on the spread of infectious diseases, we extend the *SIR* model in the present study by taking into account the nonlinear Monod-equation-type saturated incidence rate. The ratio represented by the nonlinear Monod equation is:

$$\frac{\alpha IS}{n+\beta I}, \tag{2}$$

where the illness infection force is represented by αIS, and the form of the incidence rate as a function of the infected subpopulation I is determined by n, a positive constant that denotes the degree of intervention, and β denotes the proportion of the infected population that can spread the infection further. As the proportion of people infected increases, the incidence rate rises as well, becoming independent of the number of infected subpopulations, as evidenced by the global response to the COVID-19 pandemic. This is implied by the monod equation type of incidence rate, which is low for the small number of infected segment of the population because of rigorous intervention. Figure 1 illustrates how β affects the disease's propagation, with graphs (A), (B), and (C) representing the corresponding values as $\beta = 1$, $\beta = 0.7$, and $\beta = 0.3$. The World Health Organisation (WHO) estimates the hospital bed-population ratio as the measure of resource availability to the general public. Shan and Zhu [20] took into account the effect of resource availability along with the nonlinear recovery rate that is given as follows:

$$\beta(b,I) = \beta_0 + (\beta_1 - \beta_0)\frac{b}{b+I}, \tag{3}$$

because of the quantity of available health-care resources and the proportion of infected population, β_0 and β_1, $0 < \beta_0 < \beta_1$, represent the minimum and maximum per capita recovery rates, respectively. Also, b is some positive constant that has a biological significance as it is a measure of the effect of hospital bed capacity on the spread of infectious

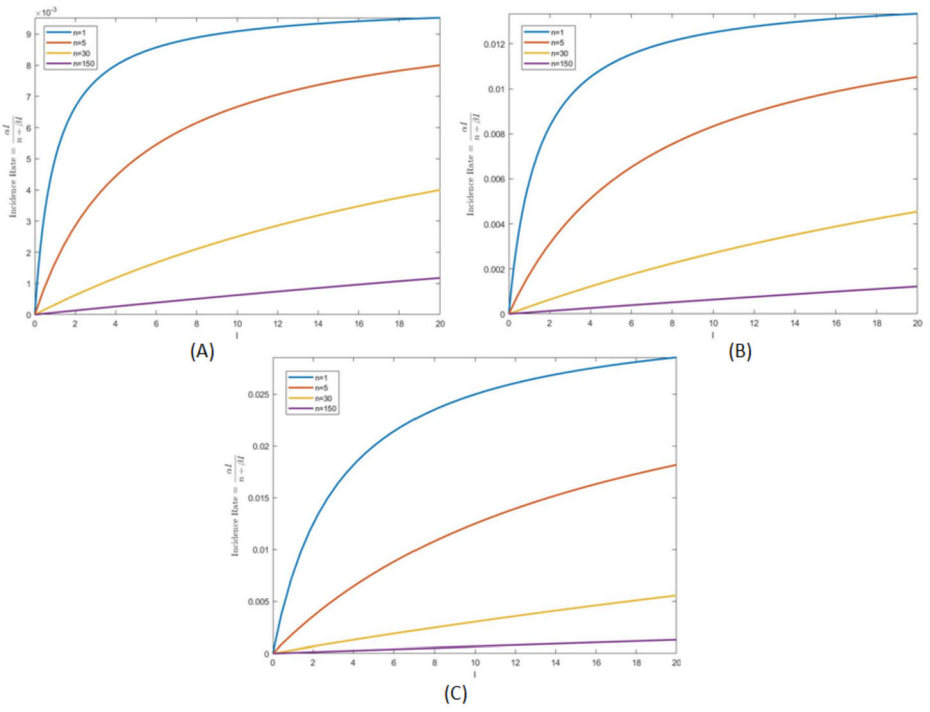

Figure 1 Impact of β on the infection rate with varying k values

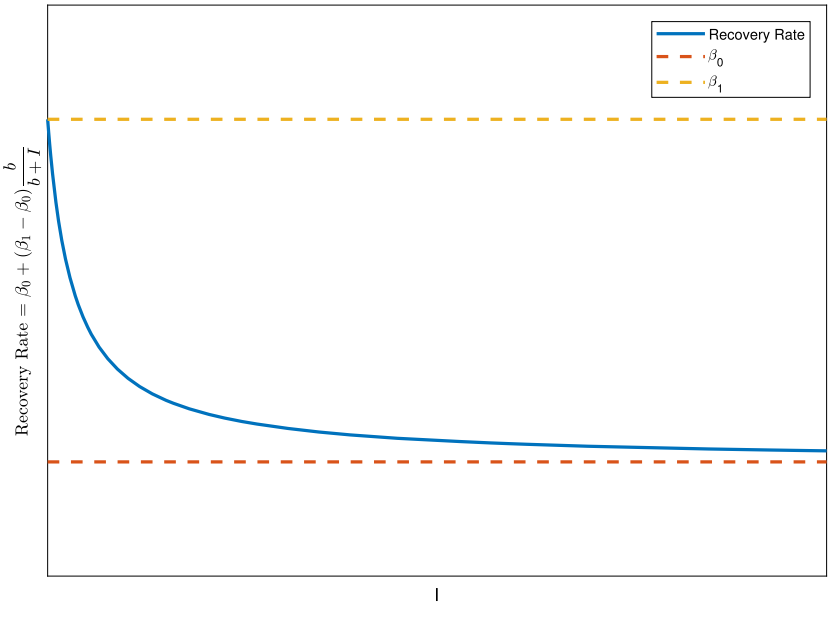

Figure 2 Graph of recovery rate for a fixed number of available resources

diseases. Figure 2 shows how the nonlinear recovery rate behaves when the quantity of resources available is known. It has been discovered that complicated dynamic behavior including forward and backward bifurcations can result from this nonlinear recovery term. Several studies conducted recently examined the infectious diseases dynamics using

various forms of incidence rates [21–24] that includes mainly two factors, infected population and intervention strategies. The presented research proposes a *SIR* model that incorporates a nonlinear saturated incidence rate and a recovery rate using a Monod-type equation. Previous researches showed that the infection rate depended on the entire population. However, this study has taken into account the possibility that an infected person might not be able to spread the infection if susceptible individuals are not available, as might be the situation under a quarantine, which makes the model novel. Furthermore, it is evident that the recovery rate is directly correlated with the quantity of resources that are accessible, such as hospital beds, oxygen cylinders, or vaccination doses, depending on the disease.

The rest of the paper is organized as follows: Following model formulation, Sect. 2 presents a mathematical validation of the model, including positivity and boundedness of the solution, basic reproduction number computation, existence of points of equilibria, bifurcation analysis, and stability analysis at equilibria points. In Sect. 3, the numerical solution is computed using the *MATLAB* solver, and the results are displayed graphically. A brief summary of the findings and the study's conclusion is given in Sect. 4.

2 Model specification

The entire population $N(t)$ is categorized into three compartments, that is, susceptible population $S(t)$, infected population $I(t)$, and recovered population $R(t)$, where, $N(t) = S(t) + I(t) + R(t)$ with individuals commuting from category $S(t)$ to category $I(t)$ at a transmission rate of $\frac{\alpha IS}{k+\beta I}$.

After acquiring the infection, a person will either recover at a rate $\beta(b, I)I$ or die at a rate γI. Since there are three subpopulations, the nonlinear dynamical system is composed of the following three nonlinear differential equations:

$$\begin{aligned}
\frac{dS}{dt} &= A - \frac{\alpha IS}{k+\beta I} - \delta S,\\
\frac{dI}{dt} &= \frac{\alpha IS}{k+\beta I} - \left(\beta_0 + (\beta_1 - \beta_0)\frac{b}{b+I}\right) I - (\gamma + \delta) I,\\
\frac{dR}{dt} &= \left(\beta_0 + (\beta_1 - \beta_0)\frac{b}{b+I}\right) I - \delta R,
\end{aligned} \tag{4}$$

where A is some positive constant that represents the birth rate, δ represents the natural mortality rate for each compartment, and γ indicates the disease-related death. The incidence rate and recovery rate are defined by Eqs. (2) and (3), respectively.

Since $R(t)$ is not present in the first two equations of system (4), it is sufficient to focus simply on the first two equations with $R(t) = N(t) - S(t) - I(t)$. The following simplified model will therefore be the main topic of discussion:

$$\begin{aligned}
\frac{dS}{dt} &= A - \frac{\alpha IS}{k+\beta I} - \delta S,\\
\frac{dI}{dt} &= \frac{\alpha IS}{k+\beta I} - \left(\beta_0 + (\beta_1 - \beta_0)\frac{b}{b+I}\right) I - (\gamma + \delta) I.
\end{aligned} \tag{5}$$

2.1 Positivity and boundedness of the solution set

Theorem 1 *The solution set*

$$\Sigma = \left\{ ((S(t)), (I(t))) \in \mathbb{R}^2_+ \cup \{(0,0)\}; S(t) + I(t) \leq \frac{A}{\delta}, \forall\, t \geq 0 \right\},$$

for the system (5) *satisfies positivity and boundedness.*

Proof Suppose that $N(t) = S(t) + I(t)$, then by adding the first two equations of system (5):

$$\frac{dN}{dt} = A - \delta N(t) - \left(\beta_0 + (\beta_1 - \beta_0) \frac{b}{b+I} \right) I - \gamma I(t),$$

implies that:

$$\frac{dN}{dt} \leq A - \delta N(t),$$

on using integration techniques, one can obtain that:

$$N(t) \leq N(0)e^{-\delta t} + \frac{A}{\delta} \left(1 - e^{-\delta t}\right).$$

Therefore, $\lim\limits_{t\to\infty} \sup N(t) \leq \frac{A}{\delta}$ and $\frac{dN}{dt} < 0$ for $N \geq \frac{A}{\delta}$. Hence, the required result holds. □

2.2 Basic reproduction number

The average number of subsequent infections that an infected person causes during the course of their infectious period when they are placed into a population that is totally susceptible is known as the basis reproduction number. Here, the next-generation matrix method [25] approach will be employed to determine the basic reproduction number, which is represented by $\Re_0$. On comparing (5) with [25], we obtain:

$$f = \frac{\alpha IS}{k + \beta I},$$
$$\nu = \left(\beta_0 + (\beta_1 - \beta_0) \frac{b}{b+I} \right) I + (\gamma + \delta) I.$$

Now, F and V will be evaluated by partial derivatives at the disease-free equilibrium point, that is:

$$F = \left.\frac{\partial f}{\partial I}\right|_{E_0}, \; V = \left.\frac{\partial \nu}{\partial I}\right|_{E_0},$$

which implies

$$F = \frac{\alpha A}{k\delta}, \; V = \beta_1 + \gamma + \delta$$

and $\Re_0$ will be the spectral radius of FV^{-1}, hence:

$$\Re_0 = \frac{\alpha A}{k\delta\,(\beta_1 + \gamma + \delta)}. \tag{6}$$

2.3 Existence of equilibria

A point of equilibrium is one where all of the state variables remain unchanged and constant. For system (5) the points of equilibria will be calculated by solving the system of equations:

$$\begin{aligned} A - \frac{\alpha IS}{k + \beta I} - \delta S = 0, \\ \frac{\alpha IS}{k + \beta I} - \left(\beta_0 + (\beta_1 - \beta_0)\frac{b}{b + I}\right) I - (\gamma + \delta) I = 0. \end{aligned} \tag{7}$$

- For disease-free equilibria, substitute $I = 0$ in (5), it is obtained that $S = \frac{A}{\delta}$, therefore:

$$E_0(S, I) = \left(\frac{A}{\delta}, 0\right).$$

- For endemic equilibria $E_1\,(S^*, I^*)$, the following equations need to be solved:

$$\begin{aligned} A - \frac{\alpha I^* S^*}{k + \beta I^*} - \delta S^* = 0, \\ \frac{\alpha I^* S^*}{k + \beta I^*} - \left(\beta_0 + (\beta_1 - \beta_0)\frac{b}{b + I^*}\right) I^* - (\gamma + \delta) I^* = 0. \end{aligned}$$

From the second equation it is obtained that:

$$S^* = \frac{(\beta_0 I^* + b\beta_1 + b\gamma + b\delta + \delta I^* + \gamma I^*)\,(k + \beta I^*)}{\alpha\,(b + I^*)}$$

and on substituting this into the first equation, it is obtained that:

$$C_1 \left(I^*\right)^2 + C_2 \left(I^*\right) + C_3 = 0, \tag{8}$$

where

$$\begin{aligned} C_1 &= (\alpha + \beta\delta)\,(\beta_0 + \gamma + \delta)\,, \\ C_2 &= b\,(\beta_1 + \gamma + \delta)\,(\alpha + \beta\delta) + \delta k\,(1 - \Re_0)\,(\beta_1 + \gamma + \delta) - \delta k\,(\beta_1 - \beta_0)\,, \\ C_3 &= bk\delta\,(1 - \Re_0)\,(\beta_1 + \gamma + \delta)\,. \end{aligned}$$

Therefore, the roots will be of the type:

$$I_1^*, I_2^* = \frac{-C_2 \pm \sqrt{(C_2)^2 - 4C_1C_3}}{2C_1}.$$

The following possible cases arise from these:

Case I When $\Re_0 < 1$, then $C_1 > 0$ and $C_3 > 0$. If $b \geq \frac{\delta k(\beta_1 - \beta_0)}{(\beta_1 + \gamma + \delta)(\alpha + \beta\delta)}$, then $C_2 > 0$, hence, (8) has no positive real roots. Else for $C_2 < 0$, equation (8) has no real root if $(C_2)^2 - 4C_1C_3 < 0$, one real and positive root if $(C_2)^2 - 4C_1C_3 = 0$, and two positive real roots if $(C_2)^2 - 4C_1C_3 > 0$.

Case II When $\Re_0 = 1$, then $C_1 > 0$ and $C_3 = 0$. Therefore, equation (8) has no real root if $b \geq \frac{\delta k(\beta_1-\beta_0)}{(\beta_1+\gamma+\delta)(\alpha+\beta\delta)}$ and only one positive real root if $b < \frac{\delta k(\beta_1-\beta_0)}{(\beta_1+\gamma+\delta)(\alpha+\beta\delta)}$. In this case one root is always zero.

Case III When $\Re_0 > 1$, clearly $C_3 < 0$ and hence $-4C_1C_3 > 0$. This implies that $\sqrt{(C_2)^2 - 4C_1C_3} > C_2$, therefore equation (8) has a unique positive real root.

2.4 Stability analysis

A stable equilibrium point is one where a minor disturbance of the solution from that equilibrium point gradually diminishes over time. Additionally, if a tiny disturbance increases over time, it is deemed unstable.

Definition 1 Assume there exists a real-valued scalar function $L(x)$ that satisfies the following:

- $L(\overline{x}) = 0$;
- $L(x)$ is positive definite for $x \neq \overline{x}$;
- $L'(x)$ is negative semidefinite along the trajectories of $x' = g(x)$.

Then, $L(x)$ is called the Lyapunov function and $\overline{x}$ is stable for the system $x' = g(x)$.

Theorem 2 *The system* (5) *at the disease-free equilibrium point* E_0 *will be locally asymptotically stable for* $\Re_0 < 1$ *and unstable when* $\Re_0 > 1$.

Proof Comparing system (5) with

$$\frac{dS}{dt} = f_1(S,I),$$
$$\frac{dI}{dt} = f_2(S,I),$$

it is obtained that:

$$f_1(S,I) = A - \frac{\alpha IS}{k+\beta I} - \delta S,$$
$$f_2(S,I) = \frac{\alpha IS}{k+\beta I} - \left(\beta_0 + (\beta_1 - \beta_0)\frac{b}{b+I}\right) I - (\gamma+\delta)I.$$

Then, the Jacobian matrix of the system (5) is denoted by J and defined as:

$$J = \begin{pmatrix} \frac{\partial f_1}{\partial S} & \frac{\partial f_1}{\partial I} \\ \frac{\partial f_2}{\partial S} & \frac{\partial f_2}{\partial I} \end{pmatrix},$$

which implies that

$$J = \begin{pmatrix} -\frac{\alpha I}{k+\beta I} - \delta & -\frac{k\alpha S}{(k+\beta I)^2} \\ \frac{\alpha I}{k+\beta I} & \frac{k\alpha S}{(k+\beta I)^2} - (\beta_0+\gamma+\delta) - \frac{b^2(\beta_1-\beta_0)}{(b+I)^2} \end{pmatrix},$$

at the disease-free equilibrium point $E_0(S,I) = \left(\frac{A}{\delta}, 0\right)$, it is obvious that:

$$J(E_0) = \begin{pmatrix} -\delta & -\frac{\alpha A}{k\delta} \\ 0 & \frac{\alpha A}{k\delta} - (\beta_1+\gamma+\delta) \end{pmatrix}.$$

Now, the characteristic equation generated from $J(E_0)$ has eigenvalues:

$$\lambda_1 = -\delta,$$
$$\lambda_2 = \frac{\alpha A}{k\delta} - (\beta_1 + \gamma + \delta).$$

Thus, the Jacobian matrix has both eigenvalues as negative if and only if $\Re_0 < 1$. Hence, by the Routh–Hurwitz criterion for stability [26], the equilibrium point E_0 is asymptotically stable for $\Re_0 < 1$ and unstable when $\Re_0 > 1$. □

Theorem 3 *The system* (5) *at the disease-free equilibrium point* E_0 *will be globally asymptotically stable for* $\frac{\alpha A}{\delta(\beta_0+\gamma+\delta)} < k$.

Proof As $\frac{\alpha A}{\delta(\beta_0+\gamma+\delta)} < k$, therefore $\Re_0 < 1$. The Lyapunov function for this problem is defined as:

$$\begin{aligned}
\frac{dL}{dt} &= \frac{dL}{dS}.\frac{dS}{dt} + \frac{dL}{dI}.\frac{dI}{dt} \\
&= \left(\frac{\delta}{A} - \frac{1}{S}\right)\left(A - \frac{\alpha IS}{k+\beta I} - \delta S\right) \\
&+ \frac{\delta}{A}\left(\frac{\alpha IS}{k+\beta I} - \left(\beta_0 + (\beta_1 - \beta_0)\frac{b}{b+I}\right)I - (\gamma+\delta)I\right) \\
&= 2\delta - \frac{\delta^2 S}{A} - \frac{A}{S} + \frac{\alpha I}{k+\beta I} - \frac{\delta}{A}\left(\gamma + \delta + \beta_0 + (\beta_1 - \beta_0)\frac{b}{b+I}\right)I \\
&\leq 2\delta - \frac{\delta^2 S}{A} - \frac{A}{S} + \frac{\left(\alpha - \frac{\delta k}{A}(\gamma+\delta+\beta_0)\right)I - \frac{\delta}{A}(\gamma+\delta+\beta_0)I^2}{k+\beta I} \\
&\leq 0,
\end{aligned}$$

because, $\beta_0 + (\beta_1 - \beta_0)\frac{b}{b+I} > \beta_0$ holds for all $I \geq 0$. Therefore, $\frac{dL}{dt} \leq 0$ holds provided that $\Re_0 \leq 1$. Also, $\frac{dL}{dt} = 0$ only at $E_0(S,I) = \left(\frac{A}{\delta}, 0\right)$, which completes the proof. □

Theorem 4 *The endemic equilibrium point* $E_1(S^*, I^*)$ *will be asymptotically stable only if equations* (9) *and* (10) *satisfy*:

$$\frac{\alpha I^*}{k+\beta I^*} + \beta_0 + \gamma + 2\delta + \frac{b^2(\beta_1 - \beta_0)}{(b+I^*)^2} > \frac{k\alpha S^*}{(k+\beta I^*)^2}, \tag{9}$$

$$\begin{aligned}
&\frac{b^2\delta(\beta_1 - \beta_0)}{(b+I^*)^2} + \delta(\beta_0 + \gamma + \delta) + \frac{b^2(\beta_1 - \beta_0)\alpha I^*}{(k+\beta I^*)(b+I^*)^2} + \frac{\alpha I^*(\beta_0 + \gamma + \delta)}{k+\beta I^*} \\
&> \frac{k\alpha\delta S^*}{(k+\beta I^*)^2}.
\end{aligned} \tag{10}$$

Proof Consider the jacobian matrix for the system (5) at the endemic equilibrium point $E_1(S^*, I^*)$:

$$J(E_1) = \begin{pmatrix} -\frac{\alpha I^*}{k+\beta I^*} - \delta & -\frac{k\alpha S^*}{(k+\beta I^*)^2} \\ \frac{\alpha I^*}{k+\beta I^*} & \frac{k\alpha S^*}{(k+\beta I^*)^2} - (\beta_0 + \gamma + \delta) - \frac{b^2(\beta_1 - \beta_0)}{(b+I^*)^2} \end{pmatrix}.$$

Then, the characteristic equation related to the matrix $J(E_1)$ will be:

$$\lambda^2 - tr\left(J(E_1)\right)\lambda + \det\left(J(E_1)\right) = 0,$$

which implies

$$\lambda^2 + H_1\lambda + H_2 = 0, \tag{11}$$

where

$$H_1 = \frac{\alpha I^*}{k+\beta I^*} + \beta_0 + \gamma + 2\delta + \frac{b^2(\beta_1-\beta_0)}{(b+I^*)^2} - \frac{k\alpha S^*}{(k+\beta I^*)^2},$$
$$H_2 = \frac{b^2\delta(\beta_1-\beta_0)}{(b+I^*)^2} + \delta(\beta_0+\gamma+\delta) + \frac{b^2(\beta_1-\beta_0)\alpha I^*}{(k+\beta I^*)(b+I^*)^2} + \frac{\alpha I^*(\beta_0+\gamma+\delta)}{k+\beta I^*} - \frac{k\alpha\delta S^*}{(k+\beta I^*)^2}.$$

Now, by applying the Routh–Hurwitz criterion it is observed that the matrix $J(E_1)$ will have eigenvalues with negative real parts if and only if both H_1 and H_2 are positive. Therefore, the equilibrium point $E_1(S^*, I^*)$ is asymptotically stable only if (9) and (10) holds. □

Theorem 5 *If we rewrite equation* (10) *as*:

$$\frac{b^2\delta(\beta_1-\beta_0)}{(b+I^*)^2} + \delta(\beta_0+\gamma+\delta) + \frac{b^2(\beta_1-\beta_0)\alpha I^*}{(k+\beta I^*)(b+I^*)^2} + \frac{\alpha I^*(\beta_0+\gamma+\delta)}{k+\beta I^*} < \frac{k\alpha\delta S^*}{(k+\beta I^*)^2},$$

then $E_1(S^*, I^*)$ *will be a saddle point. Moreover, if we rewrite equation* (9) *as*:

$$\frac{\alpha I^*}{k+\beta I^*} + \beta_0 + \gamma + 2\delta + \frac{b^2(\beta_1-\beta_0)}{(b+I^*)^2} > \frac{k\alpha S^*}{(k+\beta I^*)^2}$$

and (10) *is satisfied, then* $E_1(S^*, I^*)$ *will be unstable.*

2.5 Bifurcation analysis

A bifurcation occurs when equilibrium points undergo a shift in stability behavior or dynamics; this point of equilibrium at which a bifurcation exists is referred to as the bifurcation point.

Theorem 6 *The system* (5) *exhibits a bifurcation at the equilibrium point* $E_0(S,I) = \left(\frac{A}{\delta}, 0\right)$ *when* $\alpha = \frac{k\delta(\beta_1+\gamma+\delta)}{A}$.

Proof From $J(E_0)$, it is clear that if $\alpha = \frac{k\delta(\beta_1+\gamma+\delta)}{A}$, then one eigenvalue will be zero. Hence, the system becomes unstable at $\Re_0 = 1$. As for $\alpha < \frac{k\delta(\beta_1+\gamma+\delta)}{A}$, both the eigenvalues of the matrix $J(E_0)$ will be negative. This implies that E_0 becomes an asymptotically stable node for the system (5). Again, if $\alpha > \frac{k\delta(\beta_1+\gamma+\delta)}{A}$ holds, the matrix $J(E_0)$ has one negative and another positive eigenvalue. This implies that E_0 becomes an unstable saddle point for the system (5). Therefore, system (5) exhibits a bifurcation for $\alpha = \frac{k\delta(\beta_1+\gamma+\delta)}{A}$. □

Theorem 7 *Suppose that*:

$$\frac{\alpha I^*}{k+\beta I^*}+\beta_0+\gamma+2\delta+\frac{b^2(\beta_1-\beta_0)}{(b+I^*)^2}=\frac{k\alpha S^*}{(k+\beta I^*)^2}$$

and (10) *holds. Then, at the endemic equilibrium point* $E_1(S^*,I^*)$, *system* (5) *shows a Hopf bifurcation*.

Proof By the given condition:

$$\frac{\alpha I^*}{k+\beta I^*}+\beta_0+\gamma+2\delta+\frac{b^2(\beta_1-\beta_0)}{(b+I^*)^2}=\frac{k\alpha S^*}{(k+\beta I^*)^2},$$

it can be seen that $C_1=0$ in (11) and the equation reduces to

$$\delta^2+C_2=0.$$

Hence, by using Theorem 5, the stability behavior for the system (5) at the endemic equilibrium point $E_1(S^*,I^*)$ is totally depend on parametric value $\alpha=\alpha^*$, where:

$$\alpha^*=\frac{b^2\delta(\beta_1-\beta_0)(k+\beta I^*)^2+\delta(k+\beta I^*)^2(b+I^*)^2}{k\delta S^*(b+I^*)^2-I^*(\beta_0+\gamma+\delta)(k+\beta I^*)(b+I^*)^2-b^2I^*(\beta_1-\beta_0)(k+\beta I^*)},$$

such that

$$k\delta S^*\left(b+I^*\right)^2-I^*(\beta_0+\gamma+\delta)\left(k+\beta I^*\right)\left(b+I^*\right)^2-b^2I^*(\beta_1-\beta_0)\left(k+\beta I^*\right)\neq 0.$$

Also, we have

$$\frac{d}{d\alpha}[tr(J(E_1))]_{\alpha=\alpha^*}=\frac{kS^*-I^*(k+\beta I^*)}{(k+\beta I^*)^2}\neq 0.$$

Therefore, there exists a Hopf bifurcation for the system (5) at the endemic equilibrium point $E_1(S^*,I^*)$ for $\alpha=\alpha^*$. □

Theorem 8 *The positive quadrant of the* (S,I) *plane for the system* (5) *has no periodic solution in the interior when* $k<b\beta$.

Proof Consider a nonnegative real-valued function F such that:

$$F(S,I)=\frac{k+\beta I}{IS}>0.$$

Also, from Theorem 2, we have

$$f_1(S,I)=A-\frac{\alpha IS}{k+\beta I}-\delta S,$$

$$f_2(S,I)=\frac{\alpha IS}{k+\beta I}-\left(\beta_0+(\beta_1-\beta_0)\frac{b}{b+I}\right)I-(\gamma+\delta)I.$$

Then, we have

$$\begin{aligned} H &= \frac{\partial}{\partial S}\left(F.f_1\right) + \frac{\partial}{\partial I}\left(F.f_2\right) \\ &= -\frac{A\,(k+\beta I)}{IS^2} - \frac{\beta_0\beta}{S} - \frac{b\,(\beta_1-\beta_0)\,[b\beta-k]}{S(b+I)^2} - \frac{\beta(\gamma+\delta)}{S} \\ &< 0, \quad when \;\; k < b\beta. \end{aligned}$$

□

Hence, by using Dulac's creterion [27], it is proved that the positive quadrant of the (S, I) plane for the system (5) has no periodic solution in the interior when $k < b\beta$.

3 Numerical simulation

By the *MATLAB* solver *ode*45, which solves initial-value problems using the Runge–Kutta methods, we numerically demonstrate the results that the equilibrium point E is locally and globally asymptotically stable. Additionally, graphs for various values of β demonstrate the dynamic behavior of the susceptible and infected population. Using parametric data from Table 1, a time-dependent graph of the susceptible and infected populations was created. Table 1 makes it evident that endemic equilibrium exists at point $E^*(170.74, 2.21)$ and that the basic reproduction number is $\Re_0 = 4.2168$. Upon applying Theorem 4 to determine the validity of the parameters listed in Table 1, it is determined that the equilibrium point $E^*(170.74, 2.21)$ is locally asymptotically stable for these parametric values.

Figure 3 depicts that $S(t)$ and $I(t)$ are solutions that approach the equilibrium point $E^*(170.74, 2.21)$ and satisfy the initial condition $I(S_0, I_0) = (100, 50)$. The dynamics of the susceptible and infected populations is shown in Fig. 3 for $\beta = 1, 0.7, 0.3$, where it can be seen that every member of the infected population is actively contributing to the propagation of the infection. The graphs show the effects of various beta values on solutions S and I, these reflect the situations in which a ratio of the infected population rather than the entire infected population is available for additional infection spread. The global asymptotically stability for the endemic equilibrium point $E^*(209.91, 2.95)$ has been demonstrated using the parameter values listed in Table 2. As a result, our solutions $S(t)$ and $I(t)$ will converge to the same equilibrium point $E^*(209.91, 2.95)$ for any initial values. Figure 4 shows that the equilibrium point E is globally asymptotically stable. For the system (5), five distinct initial values have been taken into consideration in order to demonstrate the global stability of equilibrium point $E^*(209.91, 2.95)$. Figure 4 makes it abundantly evident that both solutions S and I converge to the same equilibrium point for all initial values. Additionally, using various values of k and β, the parameters listed in Table 3 have been

Table 1 Parameter values used for numerical simulation of $S(t)$ and $I(t)$

Parameter	Value	Dimension
A	1.75	individual/time
α	0.01	$(\text{individual/time})^{-1}$
k	2	individual
δ	0.005	time^{-1}
β_0	0.2	time^{-1}
β_1	0.21	time^{-1}
b	0.2	individual
γ	0.2	time^{-1}

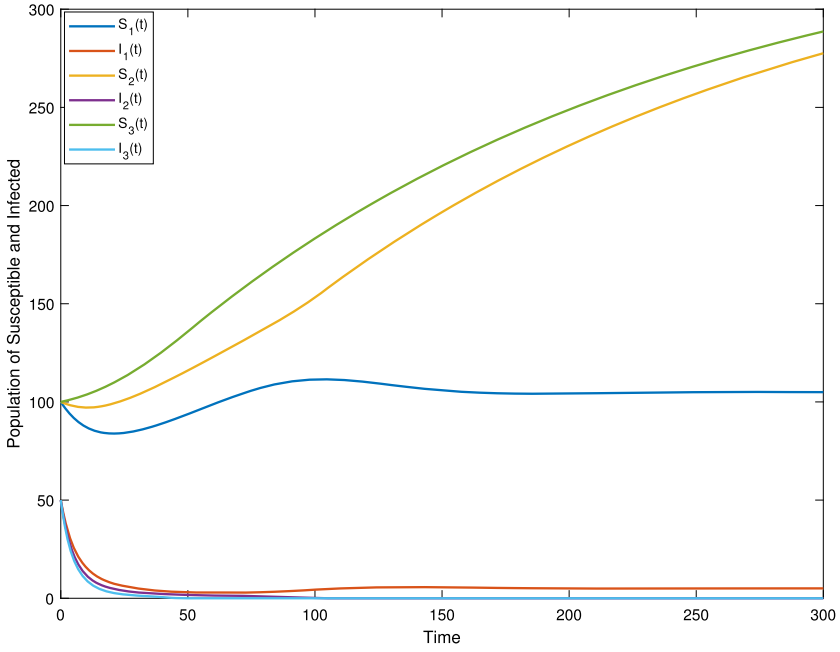

Figure 3 Relation between Susceptible and Infected Population with respect to time and $\beta = 1(S_3, I_3)$, $\beta = 0.7(S_2, I_2)$, *and* $\beta = 0.3(S_1, I_1)$

Table 2 Parameter values used for stability analysis

Parameter	Value	Dimension
A	2.3	individual/time
α	0.01	$(\text{individual/time})^{-1}$
k	2	individual
δ	0.005	time^{-1}
β_0	0.2	time^{-1}
β_1	0.5	time^{-1}
b	0.2	individual
γ	0.2	time^{-1}

utilized to model the impact of intervention levels on the propagation of infections. Using different values of k and fixed $\beta = 1$, Fig. 5 illustrates how intervention levels affect the propagation of infection. When the entire population that is affected is actively transmitting the disease, it illustrates how the infection spreads. Figure 6 shows how varying intervention levels impact the spread of infection using various values of k, which represents the level of intervention such as low, mild, moderate, and strict, and $\beta = 0.7$. It is indicative of the spread of the virus when only about 70% of the infected population is actively spreading the disease, rather than the entire infected population. Using a range of values for k, which stands for the level of intervention, including low, mild, moderate, and strict, Fig. 7 illustrates how different intervention levels affect the transmission of the infection. When just roughly 30 percent of the infected population actively spreads the disease, as opposed to the entire infected population, it represents the spread of the disease. Greater values of k indicate that employing stringent and modest therapies aids in the decrease in the number of infected individuals. The modest β values had a similar outcome.

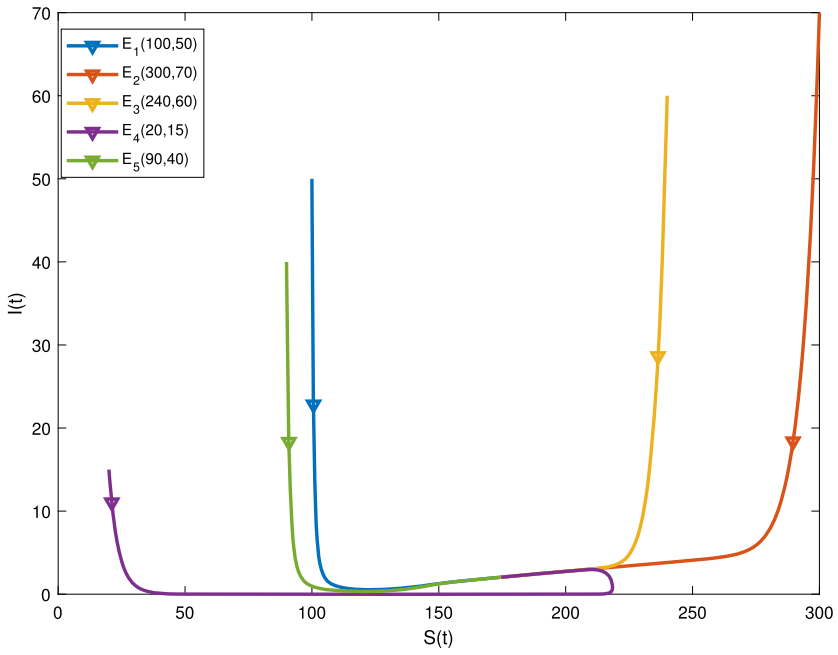

Figure 4 Stability analysis for the endemic equilibrium point E_1 with distinct initial values

Table 3 Parameters used for dynamic behavior of infected population *I*

Parameter	Value	Dimension
A	1.7	individual/time
α	0.01	$(\text{individual/time})^{-1}$
δ	0.005	time^{-1}
β_0	0.02	time^{-1}
β_1	006	time^{-1}
b	0.2	individual
γ	0.2	time^{-1}

4 Conclusion

A novel *SIR* model using a Monod-type equation featuring a nonlinear saturated incidence and recovery rate is proposed in the study. A detailed mathematical analysis has been conducted for the developed model. Firstly, the nonnegativity and boundedness of the solution set has been proved. Further, every possibility for the existence of disease-free and endemic equilibria has been discussed. Additionally, the models' dynamics are locally and it is globally analyzed. The model's stability at disease-free equilibria are explored and discovered that it was unstable when $\Re_0 > 1$ and locally and globally asymptotically stable when $\Re_0 < 1$. It is established that, for $\Re_0 > 1$, the disease endemic equilibrium E_1 (S^*, I^*) exists. Under some circumstances specified by the inequalities (9) and (10), it is locally asymptotically stable; otherwise, an unstable condition and the existence of a saddle point for the endemic equilibrium point are governed by Theorem 5. *MATLAB* has been used to carry out the numerical simulation. The use of a nonlinear incident rate as a monoid-type equation improves the study over a constant-type incident rate because the spread of infection is now determined by the force of the disease as well as the number of infected individuals available to distribute the virus. The evaluation of the recovery rate, which includes the lowest and maximum achievable recovery rates as well as the quantity

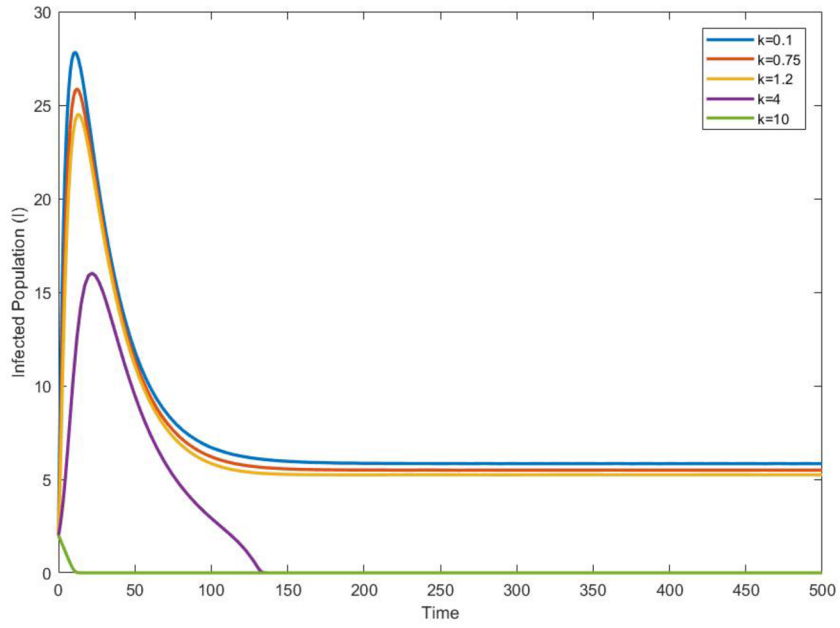

Figure 5 Dynamic behavior of Infected population (I) with varying values of k and fixed $\beta = 1$

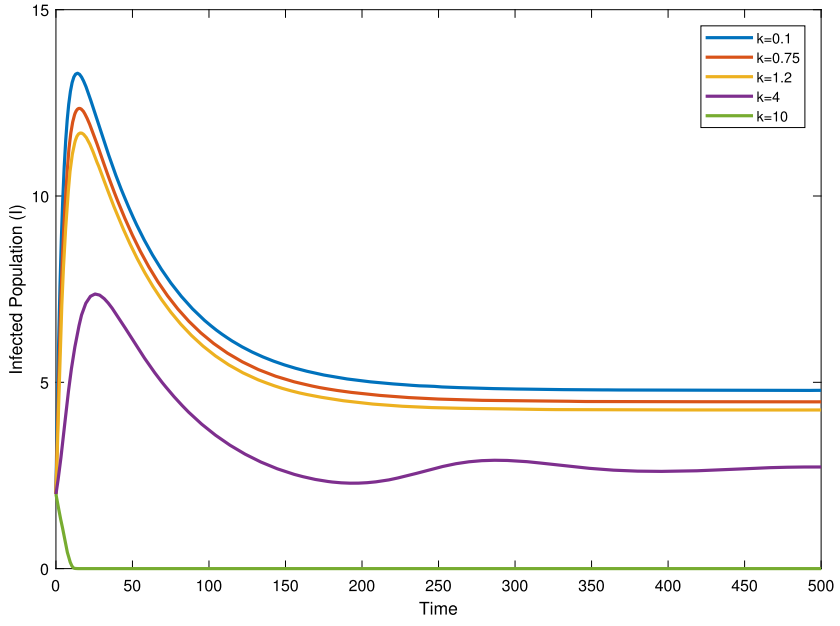

Figure 6 Dynamic behavior of Infected population (I) with varying values of k and fixed $\beta = 0.7$

of treatment resources available, improves the outcome of the research. The model's numerical simulation shows that when the rate of transmission increases, infection grows or decreases due to the availability of therapy. Furthermore, when the degree of inhibition adopted by susceptible and infected individuals grows, infection rates decrease. Based on graphical analysis, the research findings show a significant drop in the infected compart-

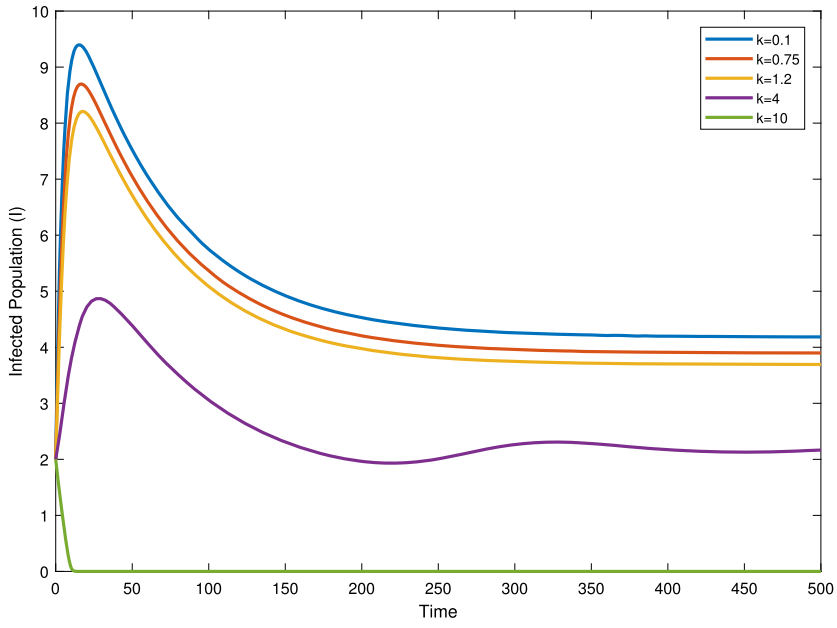

Figure 7 Dynamic behavior of Infected population (I) with varying values of k and fixed $\beta = 0.3$

ment as the preventative measure's value rises. Furthermore, the number of people who have recovered is increasing as more supplies, such as oxygen tanks, hospital beds, and doses of vaccinations, become accessible. In the future, we will focus on assessing our model's stability with various nonlinear treatment function types and incident rates. For the sake of this study, we will also consider fractional derivatives and evaluate their benefits and drawbacks.

Acknowledgements
The authors would like to thank Dr. Pranay Goswami for valuable supervision throughout the work and extend their appreciation to Taif University, Saudi Arabia, for supporting this work through project number (TU-DSPP-2024-66).

Author contributions
Each author contributed equally to the work. All authors read and approved the final manuscript.

Funding
This research was funded by Taif University, Saudi Arabia, project No (TU-DSPP-2024-66).

Data availability
Not applicable.

Declarations

Competing interests
The authors declare that they have no competing interests.

Author details
[1]School of Liberal Studies, Dr B. R. Ambedkar University, Lodhian Road, Delhi, 110006, Delhi, India. [2]Department of Science and Technology, University College Ranyah, Taif University, Ranyah, 21975, Ranyah, Saudi Arabia.

Received: 27 April 2024 Accepted: 14 January 2025 Published online: 28 January 2025

References

1. Hethcote, H.W.: The mathematics of infectious diseases. SIAM Rev. **42**(4), 599–653 (2000)
2. Anderson, R.M., May, R.M.: Infectious Diseases of Humans: Dynamics and Control. Oxford university press (1991)

3. Kermack, W.O., McKendrick, A.G.: A contribution to the mathematical theory of epidemics. Proc. R. Soc. Lond. Ser. A, Contain. Pap. Math. Phys. Character **115**(772), 700–721 (1927)
4. Kermack, W.O., McKendrick, A.G.: Contributions to the mathematical theory of epidemics. II.—the problem of endemicity. Proc. R. Soc. Lond. Ser. A, Contain. Pap. Math. Phys. Character **138**(834), 55–83 (1932)
5. Hethcote, H.W.: Qualitative analyses of communicable disease models. Math. Biosci. **28**(3–4), 335–356 (1976)
6. Agarwal, M., Verma, V.: Analysis of an sir model with saturating contact rate and carrier-dependent infectious diseases under the effect of environmental discharge. J. Int. Acad. Phys. Sci. **14**(3), 305–322 (2010)
7. Heesterbeek, J.A.P., Metz, J.A.: The saturating contact rate in marriage-and epidemic models. J. Math. Biol. **31**, 529–539 (1993)
8. Giles, P.: The mathematical theory of infectious diseases and its applications. J. Oper. Res. Soc. **28**(2), 479–480 (1977)
9. Brauer, F., Castillo-Chavez, C., Castillo-Chavez, C.: Mathematical Models in Population Biology and Epidemiology, vol. 2. Springer (2012)
10. Khan, M.A., Atangana, A.: Modeling the dynamics of novel coronavirus (2019-ncov) with fractional derivative. Alex. Eng. J. **59**(4), 2379–2389 (2020)
11. Ali, A., Alshammari, F.S., Islam, S., Khan, M.A., Ullah, S.: Modeling and analysis of the dynamics of novel coronavirus (covid-19) with Caputo fractional derivative. Results Phys. **20**, 103669 (2021)
12. Awais, M., Alshammari, F.S., Ullah, S., Khan, M.A., Islam, S.: Modeling and simulation of the novel coronavirus in Caputo derivative. Results Phys. **19**, 103588 (2020)
13. DeAngelis, D.L., Goldstein, R., O'Neill, R.V.: A model for tropic interaction. Ecology **56**(4), 881–892 (1975)
14. Beddington, J.R.: Mutual interference between parasites or predators and its effect on searching efficiency. J. Anim. Ecol., 331–340 (1975)
15. Li, G.-H., Zhang, Y.-X.: Dynamic behaviors of a modified sir model in epidemic diseases using nonlinear incidence and recovery rates. PLoS ONE **12**(4), 0175789 (2017)
16. Barrot, J., Grassi, B., Sauvagnat, J.: Sectoral effects of social distancing Covid Economics Vetted and Real-Time Papers. Issue (2020)
17. Coibion, O., Gorodnichenko, Y., Weber, M.: Labor markets during the covid-19 crisis: a preliminary view. Technical report, National Bureau of economic research, (2020)
18. Fadinger, H., Schymik, J.: The costs and benefits of home office during the covid-19 pandemic: evidence from infections and an input-output model for Germany. Covid Econ. **9**(24), 107–134 (2020)
19. Gourinchas, P.-O.: Flattening the pandemic and recession curves. Mitig. COVID Econ. Crisis: Act fast and do whatever **31**(2), 57–62 (2020)
20. Shan, C., Zhu, H.: Bifurcations and complex dynamics of an sir model with the impact of the number of hospital beds. J. Differ. Equ. **257**(5), 1662–1688 (2014)
21. Purwati, U.D., Riyudha, F., Tasman, H., et al.: Optimal control of a discrete age-structured model for tuberculosis transmission. Heliyon **6**(1) (2020)
22. Fatmawati, M.A.K., Bonyah, E., Hammouch, Z., Shaiful, E.M.: A mathematical model of tuberculosis (tb) transmission with children and adults groups: a fractional model. AIMS Math. **5**(4), 2813–2842 (2020)
23. Khan, M.A., Ullah, S., Ullah, S., Farhan, M.: Fractional order seir model with generalized incidence rate. AIMS Math. **5**(4), 2843–2857 (2020)
24. Alshammari, F.S., Khan, M.A.: Dynamic behaviors of a modified sir model with nonlinear incidence and recovery rates. Alex. Eng. J. **60**(3), 2997–3005 (2021)
25. Driessche, P., Watmough, J.: Reproduction numbers and sub-threshold endemic equilibria for compartmental models of disease transmission. Math. Biosci. **180**(1–2), 29–48 (2002)
26. DeJesus, E.X., Kaufman, C.: Routh-Hurwitz criterion in the examination of eigenvalues of a system of nonlinear ordinary differential equations. Phys. Rev. A **35**(12), 5288 (1987)
27. McCluskey, C.C., Muldowney, J.S.: Bendixson-dulac criteria for difference equations. J. Dyn. Differ. Equ. **10**, 567–575 (1998)

Publisher's Note